https://doi.org/10.5194/egusphere-2023-2037
Preprint. Discussion started: 19 September 2023

Significant human health co-benefits of African emissions mitigation

Christopher D. Wells[1,2], Matthew Kasoar[3], Majid Ezzati[4,5,6], Apostolos Voulgarakis[3,7]

[1]The Grantham Institute for Climate Change and the Environment, Imperial College London, London, UK.
[2]School of Earth and Environment, University of Leeds, Leeds, UK.
[3]Leverhulme Centre for Wildfires, Environment and Society, Department of Physics, Imperial College London, London, UK.
[4]Department of Epidemiology and Biostatistics, School of Public Health, Imperial College London, London, UK.
[5]MRC Centre for Environment and Health, School of Public Health, Imperial College London, London, UK.
[6]Regional Institute for Population Studies, University of Ghana, Accra, Ghana.
[7]School of Environmental Engineering, Technical University of Crete, Chania, Greece.

Correspondence to: Christopher D. Wells[1] (c.d.wells@leeds.ac.uk)

Abstract. Future African aerosol emissions, and therefore air pollution levels and health outcomes, are uncertain. Here, the range in the future impacts of African emissions in the Shared Socioeconomic Pathway (SSP) scenarios is studied, using the Earth System Model UKESM1 along with human health concentration-response functions. Using present-day demographics, annual deaths attributable to ambient particulate matter are estimated to be lower by 150,000 under stronger African aerosol mitigation by 2090, while those attributable to O_3 are lower by 15,000. The particulate matter health benefits are realised predominantly within Africa, with the O_3-driven benefits being more widespread – though still concentrated in Africa – due to the longer atmospheric lifetime of O_3. These results demonstrate the important health co-benefits from future emissions mitigation in Africa.

1 Introduction

Anthropogenic emissions of aerosols, their precursors, and reactive gases have substantial impacts on the climate. These impacts include a general aerosol cooling and, to a lesser extent, warming due to tropospheric O_3 (C. J. Smith et al., 2020; Thornhill et al., 2021), as well as shifts in circulation patterns such as monsoons (Kasoar et al., 2018; Liu et al., 2018; Shawki et al., 2018; Wang et al., 2016). In addition to their climate effect, aerosols contribute to fine particulate matter air pollution, termed $PM_{2.5}$ to denote particles with diameters less than 2.5μm (S. Turnock et al., 2020) . Reactive gases also modify concentrations of O_3, another important climate forcer and air pollutant (von Schneidemesser et al., 2015). Due to their relatively short lifetimes, the effects of aerosols on the climate and human health depends on their emission location (Persad & Caldeira, 2018), with the health impact being particularly localised (Shindell et al., 2018). Since these species are co-emitted with greenhouse gas emissions, general climate change mitigation policies can lead to health co-benefits via reduced air pollution (Shindell et al., 2018).

Global $PM_{2.5}$ concentrations have increased 15-20% since the pre-industrial era to 6.9 ± 1.5 μg m^{-3} (S. Turnock et al., 2020) , and are thought to still be slightly increasing in recent decades by 0.2% yr^{-1}, particularly over Asia and southern Africa (Gliß

https://doi.org/10.5194/egusphere-2023-2037
Preprint. Discussion started: 19 September 2023

et al., 2021). The average concentration experienced by humans is much higher than this global average due to the co-location of anthropogenic sources with population centres; 69% of people are estimated to be exposed to $PM_{2.5}$ concentrations higher than 10 μg m^{-3} (Lelieveld et al., 2013), with an average population-weighted $PM_{2.5}$ exposure of 38 μg m^{-3}, reducing to just 11 μg m^{-3} when excluding fossil fuel emissions (Vohra et al., 2021). The World Health Organisation recommends limiting long-term exposure to less than 5 μg m^{-3} (World Health Organisation, 2021), lowered in 2021 from their previous threshold of 10 μg m^{-3}, though there is no known safe level of $PM_{2.5}$ concentrations (Silva et al., 2013). Present-day human health impacts of $PM_{2.5}$ are substantial but uncertain, with estimates varying from 2.37 (1.33 – 2.93) million deaths yr^{-1} (Partanen et al., 2018) to the more recent finding of 8.7 (-1.8 – 14.0) million deaths yr^{-1} (Vohra et al., 2021). In other studies, 3.61 (2.96-4.21) million deaths yr^{-1} have been attributed to fossil-fuel $PM_{2.5}$ alone (Lelieveld et al., 2019), and the Global Burden of Disease 2019 (hereafter: GBD2019) estimated $PM_{2.5}$-attributable deaths to be 4.14 (3.55 – 4.80) million deaths yr^{-1} (GBD 2019 Risk Factors Collaborators, 2020).

Anthropogenic activity has also increased surface concentrations of O_3, by 11.7ppb to the present-day levels of 29.9ppb (S. Turnock et al., 2020). O_3's lifetime is longer than that of $PM_{2.5}$, but its effects are still strongly co-located with anthropogenic activity, with a population-weighted concentration of around 57ppb (Anenberg et al., 2010). Impacts of O_3 on premature mortality have been estimated to be 0.7 ± 0.3 million deaths yr^{-1} (Anenberg et al., 2010) and 0.38 (0.12 – 0.73) million deaths yr^{-1} (Silva et al., 2016), using the same concentration-response functions (CRFs) (Jerrett et al., 2009). Using more recent CRFs (Turner et al., 2016) 0.6 ± 0.1 million deaths yr^{-1} were attributed to O_3-linked respiratory causes (Shindell et al., 2018), and GBD2019 attributed 0.365 (0.175-0.504) million deaths yr^{-1} to O_3, purely from Chronic Obstructive Pulmonary Disease (COPD) (GBD 2019 Risk Factors Collaborators, 2020).

Future impacts of air pollutants will depend on both emissions and demographic changes. The reduced air pollution from measures targeting the direct lowering of carbon emissions rather than relying on negative emissions technologies would prevent 93 ± 41 million deaths from $PM_{2.5}$ and 60 ± 18 million deaths from O_3 over the 21st century (Shindell et al., 2018). Measures compatible with 2oC warming are projected to reduce life-years lost due to $PM_{2.5}$ by 0.7 million yr yr^{-1} in Europe by 2050 compared to a business-as-usual scenario, despite population increases (Schucht et al., 2015). Air pollutant emissions decrease into the future in all the CMIP5-era Representative Concentration Pathway (RCP) scenarios, with reduced future air pollution-linked mortality (Silva et al., 2016). However, the range in aerosol emissions between the different RCP scenarios is far smaller than that covered by the newer Shared Socioeconomic Pathways (SSPs) (M. J. Gidden et al., 2019), which extend the RCP framework to include different socioeconomic and demographic trends, and are projected to have substantially different air pollution impacts on human health (Im et al., 2023). Thus, the future range of possible human health impacts of air pollution is larger under more recent, less explored, scenarios.

Several previous studies have investigated the human health impacts of changes in global emissions, but predominantly consider the global response. The effect of the newer SSPs on human health has also yet to be studied in detail, with the latest

https://doi.org/10.5194/egusphere-2023-2037
Preprint. Discussion started: 19 September 2023

CRFs. The continent of Africa features a complex mix of air pollutant sources, both natural and anthropogenic, with a broad range in future emissions pathways, some of which involve drastic increases in pollutants in key regions (S. Turnock et al., 2020). The wide range in potential future African air pollutant emissions suggests concurrently disparate possible air pollution impacts over the continent. Despite this, Africa has been historically understudied, especially in exposure-response cohort studies (Chen & Hoek, 2020). Nevertheless, the recent inclusion of high air pollution cohort studies from the Global South in recent CRFs (e.g. (R. Burnett et al., 2018; GBD 2019 Risk Factors Collaborators, 2020)), allows for a more accurate investigation of the effect of air pollution on human health in Africa than previously possible.

The current study investigates the potential future impacts of African emissions on air pollution, both within and beyond the continent. A strong mitigation control scenario (Shared Socioeconomic Pathway SSP119; see Section 2 and Figure S1) is compared to three experiments with a subset of African aerosol and reactive gas emissions substituted for those from a weak mitigation scenario (SSP370). These three experiments use in turn emissions of aerosol and reactive gas from the weak mitigation scenario from three different sources: biomass burning (BB), non-BB, and all sources. The experiments are named for the emissions which are substituted from SSP370, and are thus termed AerBB, AerNonBB, and AerAll respectively. AerNonBB features higher African non-BB emissions than the control, while BB emissions from Africa in AerBB are relatively reduced (Figure S1). N.B. the terminology non-BB is used in this paper to refer to the non-biomass burning emissions themselves (i.e. those from fossil fuels and biofuels), which are changed in both AerAll and AerNonBB, and so the effects of changed non-BB emissions are found under both experiments. BB similarly refers to biomass burning emissions, changed in both AerAll and AerBB. NonBB emissions are purely anthropogenic, while those from biomass burning are complexly related to human activity, particularly over Africa (Bauer et al., 2019), driving the counterintuitive increase in BB emissions in the stronger mitigation scenario. The UK Earth System Model 1 (UKESM1) is used to simulate the climate response to each emissions scenario. Ten control experiments are used, identical in their emissions but driven with different initial conditions to explore the internal variability (see Section 2); seven realisations of each of the three additional scenarios are simulated. Pollutant concentrations are not bias-corrected here, in order to determine the specific estimation in UKESM1 and due to the sparse observations over Africa. The focus is therefore on the relative impact of the scenarios, while also contextualising the magnitudes in relation to prior studies.

The control scenario thus depicts a global future with strong climate mitigation policies, leading to relatively low greenhouse gas emissions and consequently low air pollutant levels. Each of the alternative scenarios represents a future in which Africa instead follows a weak mitigation scenario in its emissions of air pollutant precursors, allowing for an exploration of the health impacts of such a range in future trajectories. Present-day population and baseline mortality rates are used throughout, to isolate the effect of changing air pollutants (see Section 2).

https://doi.org/10.5194/egusphere-2023-2037
Preprint. Discussion started: 19 September 2023

2 Methods

2.1 Model and Experiments

This study uses the UK Earth System Model version 1 (UKESM1), a fully-coupled global climate model used in the CMIP6 model intercomparison exercise. UKESM1 couples the ocean module NEMO to its atmospheric module GA7.1 and the land module GL7, with further couplings to earth system components such as the biogeochemical scheme (Sellar et al., 2019). Its horizontal resolution is 1.875° × 1.25°, with 85 vertical levels. The atmospheric scheme features interactive chemistry, with 291 reactions and 84 species (Archibald et al., 2020). This is coupled to the GLOMAP-mode aerosol scheme, which simulates the concentrations of Black Carbon (BC), Organic Carbon (OC), Sulfate, sea salt, Primary Marine Organic Aerosol (PMOA), and Secondary Organic Aerosol (SOA) in five lognormal modes, four soluble and one insoluble(Bellouin et al., 2013; Mulcahy et al., 2020). GLOMAP-mode is a 2-moment scheme, calculating both aerosol mass and number concentration, allowing different processes to impact these independently. Dust is treated separately within UKESM1 via the older 1-moment (mass only) CLASSIC scheme (Bellouin et al., 2011).

UKESM1's representation of surface $PM_{2.5}$ and O_3 has been evaluated in relation to observations and other models (S. Turnock et al., 2020) (in particular, Figures 3-8 in (S. Turnock et al., 2020)). In areas that are well-sampled with surface $PM_{2.5}$ measurements, UKESM1 is consistent with other CMIP6 models, exhibiting a low-bias in $PM_{2.5}$ in Eastern Europe and North America by around 2-10μg m^{-3}. Over oceans $PM_{2.5}$ is also systematically low, but the picture over other land areas is mixed, compared to MERRA reanalysis. In the multi-model mean, $PM_{2.5}$ concentrations over Northwest Africa are too low (S. Turnock et al., 2020), while those over East and Southern Africa are too high, by around 2-15 μg m^{-3} between models. Concentrations over Asia are also generally too high, with all bias patterns roughly similar between DJF and JJA. UKESM1 is typical in its $PM_{2.5}$ bias across most regions, including northern Africa. In Sub-Saharan Africa, however, it exhibits a stronger seasonal cycle than other models, with the main biomass burning seasons featuring substantially higher $PM_{2.5}$ concentrations than other models and the observational best estimate. Simulated $PM_{2.5}$ concentrations are up to 50% higher than the multi-model and observational means in July and January, though they still lie close to the wide observational range. The areas of high biases in CMIP6 are areas with high background $PM_{2.5}$ and large ranges in simulated concentrations across CMIP6, with inter-model standard deviations of over 20μg m^{-3} in the most polluted areas of northern and central Africa.

CMIP6 models generally exhibit high-biases in surface O_3, overestimating North American, European, and East Asian concentrations by around 10ppb in DJF and JJA compared to surface observations (S. Turnock et al., 2020). UKESM1 has typical biases in JJA (i.e. high), but overestimates the amplitude of the seasonal cycle becoming the only one of five CMIP6 models studied by (S. Turnock et al., 2020) to exhibit a low bias over Northern Hemispheric land. As for $PM_{2.5}$, the areas with the largest concentrations and inter-model standard deviations are the high emissions regions in Africa and Asia. UKESM1's

https://doi.org/10.5194/egusphere-2023-2037
Preprint. Discussion started: 19 September 2023

representation of O_3 over Sub-Saharan Africa is much closer to the multi-model mean; the lack of local surface observations precludes a full evaluation, though the sole observational station in South Africa closely tracks the models' regional averages (Figure 4 in (S. Turnock et al., 2020)).

Aerosol Optical Depth (AOD) in UKESM1 is consistent with satellite observations in low-AOD areas, but is low-biased over some areas with strong aerosol emissions such as West Africa (Mulcahy et al., 2020).

This study uses the Shared Socioeconomic Pathway (SSP) emissions trajectories to estimate the future health impact of different African emissions pathways. The SSPs are denoted SSPx-y, with x an integer referring to one of five socioeconomic narrative pathways, to explore different non-climate societal evolutions, and y denoting the top-of-atmosphere (TOA) radiative forcing in 2100 under a particular mitigation scenario (O'Neill et al., 2017). The SSPs therefore explore a range of future possible trajectories covering both socioeconomic and mitigation trends. This project uses SSP119 as a control scenario. Designed to be roughly consistent with strong mitigation under the Paris agreement, this follows socioeconomic trajectory 1 – "sustainability" (van Vuuren et al., 2017) – along with broad emissions reductions to approximately reach 1.9 W m^{-2} radiative forcing in 2100. To test the effect of weaker mitigation in Africa for different sets of emissions, three experiments are simulated, switching out the SSP119 aerosol and reactive gases emissions over Africa for their SSP370 equivalent. SSP370 follows the socioeconomic trends in narrative 3 – "regional rivalry" (Fujimori et al., 2017) – coupled with weak mitigation, leading to a TOA radiative forcing of 7 W m^{-2} in 2100. The three experiments performed are named after the SSP370 emissions subset which is substituted over Africa, and are:

AerAll
AerNonBB
AerBB

AerAll indicates that all aerosol and reactive gas emissions over Africa are substituted with SSP370, while emissions over all other areas, and for other climate forcers such as well-mixed GHGs over Africa, are kept at their SSP119 values as in the control. AerBB then switches out just the biomass-burning (BB) components of aerosols and reactive gases, and AerNonBB changes only the non-BB emissions (i.e. fossil fuel and biofuel) over Africa.

The aerosol emissions changed are BC and OC, and the reactive gases are C_2H_6, C_3H_8, CO, dimethyl sulfide (DMS), HCHO, Me_2CO, MeCHO, NH_3, NO, lumped non-methane volatile organic compounds (NVOC), and SO_2. In UKESM1, all these emissions species have both BB and non-BB components except for SO_2, which has only a non-BB component. All are emitted from the surface except a subset of BB BC and OC representing large fires, which are injected vertically uniformly from the surface to 3km, and aircraft NO emissions which are injected in a 3D grid. It should be noted that, since the aerosol and O_3 precursors are co-emitted with greenhouse gases, these scenarios changing emissions subsets are not realistic future scenarios.

https://doi.org/10.5194/egusphere-2023-2037
Preprint. Discussion started: 19 September 2023

Instead, the purpose is to investigate the range of plausible human health impacts between scenarios, which are driven by the species altered in these experiments.

Multiple ensemble members were simulated for each experiment, each initiated in 2015 with slightly different atmospheric and ocean conditions to explore the internal climate variability. Ten ensemble members of SSP119 are used for the control – five simulated for this study and five taken from the UKESM1 CMIP6 experiments, and seven of each of the other experiments are simulated. All simulations run the length of the SSP scenarios, i.e. 2015-2100. The analysis of the health impacts here focuses on the effects in 2090. For the O_3 impacts, the five UKESM1 CMIP6 control members didn't output the concentrations hourly, so only the five control experiments simulated for this project were used for the control concentrations. The local and remote climate impacts of these emissions scenarios, plus additional scenarios changing CO_2 emissions similarly, are explored in a separate paper (Wells et al., 2023).

Figure S1 indicates the time evolution of the aerosol and SO_2 emissions over Africa and globally in the control (black) and experiments (red), with total and BB carbonaceous aerosol shown. Also shown is maps of the emissions differences for carbonaceous aerosol and SO_2. Total carbonaceous aerosol emissions over Africa decline quickly in the SSP119 control, consistent with general emissions mitigation, whereas they remain roughly flat in SSP370. This acts to dampen the general global decrease in emissions, though they still almost halve at the global level through the 21st century as the rest of the world follows SSP119. The BB emissions subset, however, shows the opposite (and weaker) trend, with emissions remaining approximately constant in SSP119 but declining in SSP370, while global emissions decline in each case. This is inconsistent with the general emissions reductions in SSP119, and is reflective of the more complex link between anthropogenic activity and BB emissions than between human actions and non-BB emissions. Different IAMs were used to produce the emissions pathways for the different scenarios (IMAGE for SSP1 and AIM/GCE for SSP3 (Fujimori et al., 2017; van Vuuren et al., 2017)); this makes a clear understanding of the differences between complex emissions sources difficult, but it likely relates to different land-use activity in the scenarios. Non-BB emissions still dominate the carbonaceous aerosol emissions change, as indicated by the larger overall carbonaceous emissions in SSP370 than SSP119 over Africa. The SO_2 emissions change features a complex pattern, with higher emissions across most of the continent in SSP370 than SSP119, but relatively lower over southern Africa (except South Africa). In both cases, emissions drop overall substantially, and the differing spatial changes over Africa approximately cancel to drive little overall emissions difference between the scenarios. As with the BB aerosol changes, the specific cause of the differing trends in SO_2 emissions is hard to discern, though it is driven by stronger industrial SO_2 emissions in SSP119 (M. Gidden et al., 2018), indicating a projected faster industrialisation in SSP119 than SSP370 in southern Africa.

2.2 Health Impact Analysis

https://doi.org/10.5194/egusphere-2023-2037
Preprint. Discussion started: 19 September 2023

Many studies utilise a common methodology to estimate the human health impact of a given concentration, or change in concentration, of pollutants (e.g. (Anenberg et al., 2010; Shindell et al., 2018)). Cohort studies, tracking a large population over many years, are used to produce empirically-determined concentration-response functions (CRFs), linking background air pollutant concentrations to the change in the Relative Risk (RR) of dying from a particular Cause Of Death (COD). The RR at zero concentration is one by definition, and increases monotonically above a Low Concentration Threshold (LCT). The form of RR is constrained by the fit used to derive the function. Early studies used exponential fits (Pope III et al., 2002), while others use linear relationships or power laws (Ezzati et al., 2004; Pope III et al., 2009), while more recent studies use more complex functional forms (R. Burnett et al., 2018; R. T. Burnett et al., 2014).

While various cofounding factors are controlled for – such as lifestyle and income level – it is not necessarily valid to generalise a RR from a single cohort to the global scale. This issue especially applies to the extrapolation of pollutant concentrations to levels outside those experienced by the cohort population. In particular, a large American Cancer Society cohort study was used to generate earlier RR curves, but the highest $PM_{2.5}$ concentrations this cohort was exposed to were less than 30 μg m^{-3}, lower than the global population-weighted average of 38 μg m^{-3} found by (Vohra et al., 2021). This gap can be bridged using data from active smoking, but this assumes a short, high exposure burst – from smoking individual cigarettes – has the same health effect as a lower, continuous background concentration (Pope III et al., 2009; K. R. Smith & Peel, 2010). More recent studies use multiple cohort studies across a range of ambient exposures, significantly mitigating this issue (R. Burnett et al., 2018; GBD 2019 Risk Factors Collaborators, 2020), and rendering such CRFs more applicable to highly-polluted regions than prior estimates. At the other end of the exposure range, the assumed LCT below which the RR is one (i.e. pollutant concentrations below this have no human health effect) has decreased in consecutive studies, as cohorts in ever cleaner environments still exhibit significant effects of air pollution; there is no biological justification for a threshold, and more recent CRFs, including that used here, use a statistical distribution to represent the LCT (GBD 2019 Risk Factors Collaborators, 2020).

The "Attributable Fraction" (AF) estimates the fraction of deaths – of a particular COD – attributable to the air pollutant exposure (Mansournia & Altman, 2018):

$$\mathrm{AF} = (\mathrm{RR} - 1)/\mathrm{RR} = 1 - (1/\mathrm{RR}). \qquad (1)$$

Given a COD-specific RR curve, and common grids of surface concentrations of the pollutant (either $PM_{2.5}$ or O_3), baseline population (Pop), and mortality for a specific COD (y0), the number of deaths attributable to the pollutant can be estimated as

$$\mathrm{Deaths} = \mathrm{y0} * \mathrm{Pop} * \mathrm{AF}. \qquad (2)$$

https://doi.org/10.5194/egusphere-2023-2037
Preprint. Discussion started: 19 September 2023

Equation 2 is applied at each gridcell to determine the estimated annual deaths within the cell.

The Concentration-Response Functions used in this study are taken from the Global Burden of Disease 2019 (hereafter: GBD2019) (GBD 2019 Risk Factors Collaborators, 2020) for $PM_{2.5}$, and from (Turner et al., 2016) for O_3. While studies prior to GBD2019 imposed functional forms of varying complexity on their CRFs, GBD2019 uses a Bayesian Meta-Regression method to provide the fit, with only the assumption that the CRF should be monotonic. Due to the uncertainties regarding the existence and level of safe low concentrations of $PM_{2.5}$, GBD2019 suggests the use of a uniform distribution from 2.4-5.9 μg m^{-3} for the LCT, representing the lowest and the 5th percentile concentrations found in the background concentrations – this threshold is used in this study. The GBD2019 dataset provides 1000 "draws" of the fit for each COD-age pair, with no threshold; an LCT from the suggested uniform distribution was then randomly selected for each draw to complete the distribution.

GBD2019 provides CRFs for six CODs for $PM_{2.5}$: Lung Cancer (LC), Chronic Obstructive Pulmonary Disease (COPD), Lower Respiratory Infection (LRI), Type 2 Diabetes (T2DM), Stroke, and Ischemic Heart Disease (IHD). The latter two are age-dependent, on 5-year brackets; T2DM applies only to populations over 25 years; and the other CODs are applied to the total population. The CRFs for $PM_{2.5}$ apply to annual average $PM_{2.5}$ concentrations.

Following prior studies (GBD 2019 Risk Factors Collaborators, 2020; Malley et al., 2017; Shindell et al., 2018), the CRF for O_3 in this study was taken from (Turner et al., 2016) for respiratory mortality, which includes COPD, LRI, upper respiratory infections, asthma, pneumoconiosis, interstitial lung disease, pulmonary sarcoidosis, and other chronic respiratory diseases. This CRF applies to populations over 30, and applies to the annual average of the daily maximum 8-hour mean concentration. An LCT of 26.7ppb, the minimum concentration found in the cohort studies used by (Turner et al., 2016) is applied here, with a sensitivity test carried out applying an LCT of 31.1ppb, representing the 5th percentile in the underlying cohort data.

This study uses the following approximation for $PM_{2.5}$:

$$PM_{2.5} = OC + BC + SO_4 + 0.25 * SS + 0.1 * Dust. \quad (3)$$

i.e. all carbonaceous and sulfate aerosol contributes to $PM_{2.5}$, but only 25% of sea salt and 10% of dust are assumed to be less than 2.5μm in diameter. This approximation is used in AerChemMIP (S. Turnock et al., 2020) and other studies (e.g. (Allen et al., 2021)).

Single years of pollutant concentrations, averaged across the ensembles, were utilised in this study – 2015, 2050, and 2090. There are several reasons for the choice to use single years rather than e.g. averaging over a decade to smooth out interannual

https://doi.org/10.5194/egusphere-2023-2037
Preprint. Discussion started: 19 September 2023

variability. The present-day value needed to be centred around 2015, the start of the scenarios, since this is where the emissions start to diverge. All simulations were initialised from 2015, so it wouldn't have been possible to use a larger window to average around 2015. If data past 2015 had been used, e.g. 2015-2025 for the present day, this would have introduced other issues: since the emissions scenarios diverge from 2015, the choice of scenario to take the data from would affect the results, and this wouldn't represent the present-day in the other scenarios; in addition, the rapid decrease in emissions from 2015 in all scenarios would mean the 2015-2025 average would be significantly lower than the concentrations in 2015, and therefore not closely represent the conditions experienced by the 2015 population distributions present-day concentrations.

Population numbers from the SSPs in 2015 – equal between scenarios since the SSPs only diverge after 2015 – were used to ensure consistency across the methodology (Lutz et al., 2018). Equation 2 is applied in each model grid-cell level, using the pollutant concentrations output from UKESM1, so the country-level population data was re-gridded to the 1.875° × 1.25° UKESM1 grid. To approximately preserve present-day within-country population distributions, a high resolution (0.25° × 0.25°) present-day population file was used (CIESIN, 2018), and a country name was assigned to each cell within this grid using a global shapefile (Sandvik, 2008). The present-day population distribution within each country was then scaled to create the correct total for each age-year pair, and these distributions were then re-gridded to the UKESM1 grid resolution. Baseline mortality data for each COD-age pair was applied at the country-level (IHME, 2020), and re-gridded to the UKESM1 grid using the global shapefile.

Present-day populations were used for the analysis for two reasons. First, to isolate the effect of changes in emissions on human health. Second, while the SSPs include population projections, they do not include future baseline mortality estimates, and present-day mortality rates cannot be assumed constant while populations and other social factors change significantly, and differently between scenarios.

3 Results

3.1 Air Pollution Impact

Africa is a continent with a major presence of key pollutants compared to the global average, as seen in Figure S2. Based on our UKESM1 simulations, the organic carbon (OC) contribution to $PM_{2.5}$ is generally highest in the tropical biomass burning regions, peaking in Africa; this is also true for atmospheric dust. The distribution of O_3 is smoother than that of $PM_{2.5}$, owing to its longer lifetime, with the concentrations again being higher than average near the main emissions regions, in the low latitudes in Africa.

https://doi.org/10.5194/egusphere-2023-2037
Preprint. Discussion started: 19 September 2023

The changes in surface $PM_{2.5}$ and O_3 over Africa near the end of the century (2090) for all simulations, split into contributions from each component, are shown in Figure 1. Figure S3 shows the corresponding timeseries of simulated pollutants for Africa, its sub-region west Africa, neighbouring region Europe, as well as for the whole globe. The simulations explore the change in pollution levels in scenarios where the whole globe follows a strong mitigation pathway, while Africa follows a more "pessimistic" policy pathway in terms of its biomass burning aerosols (AerBB simulation; though as discussed in Section 2 these emissions are higher in the control), non-biomass burning aerosols (AerNonBB) and all aerosols combined (AerAll) (see Section 2). The carbonaceous aerosol increases under AerNonBB are near the main non-biomass burning emission regions, especially in West and East Africa, while reductions under AerBB are centred on the biomass burning regions North and South of the Equator. AerAll then exhibits features of both. Sulfate shows weaker changes, with the North African non-BB increased emissions contrasting with the reduced emissions south of the Equator. Changes in dust are significant, with a substantial decrease in areas with high background dust emissions. This decrease in dust emissions is ultimately due to the impact of the aerosol emissions on local surface winds, which drives the emission of dust (See Figure S4 in the Supplement). O_3 follows a similar pattern to the $PM_{2.5}$ changes, as its concentration is modified by the reactive gases co-emitted with the anthropogenic aerosol species.

https://doi.org/10.5194/egusphere-2023-2037
Preprint. Discussion started: 19 September 2023

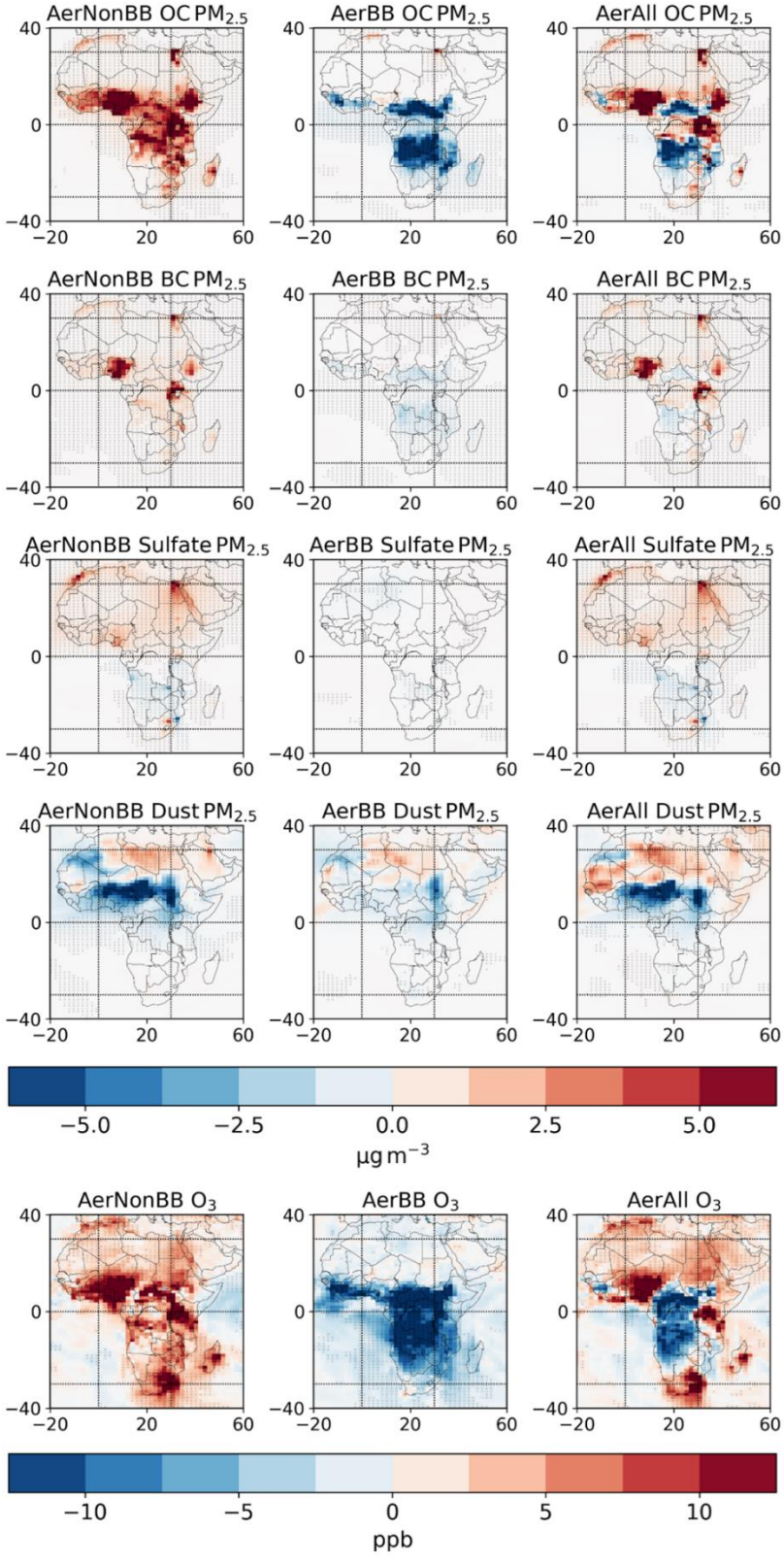

315

https://doi.org/10.5194/egusphere-2023-2037
Preprint. Discussion started: 19 September 2023

Figure 1: The change in the organic carbon (OC), black carbon (BC), sulfate, and dust aerosol contributions to surface $PM_{2.5}$, and O_3, under each emissions scenario relative to the SSP119 control in 2090 over Africa. Stippling indicates areas where the ensemble mean change is greater than one intra-ensemble standard deviation away from zero.

3.2 Health Impact

The estimated deaths in 2015 from $PM_{2.5}$ (6 Causes of Death (CODs), see Section 2) and O_3 (respiratory illnesses only) per 1000km^2 are shown in the top row of Figure 2. Table 1 indicates global and regional totals. The control SSP119 experiment is used for the air pollutant concentrations in 2015, an arbitrary choice as the SSP emissions diverge only after this year.

Globally, 2.76 (2.11 – 3.48) million annual deaths are attributed to $PM_{2.5}$, with Ischemic Heart Disease (IHD) the largest COD followed by Stroke, and 2.28 (1.73 – 2.70) million to O_3. Deaths are highest in areas where population densities and pollutant concentrations are high: in East and South Asia, and in tropical Africa. The highest number of deaths attributable to $PM_{2.5}$ and O_3 exposure occur in Asia; Africa experiences large impacts too – 12% and 7.4% of the global total for $PM_{2.5}$ and O_3 respectively.

The methodology of this study is not directly comparable to comprehensive estimates of the present-day impact of air pollution, since only one model with no bias correction is used here; the focus of the analysis is on the differences between scenarios instead. However, the magnitude of the estimated impacts can be contextualised against prior studies to explore the effect of these methodological differences. Our estimate for total present-day $PM_{2.5}$-related deaths is generally lower than prior studies; its central estimate is lower than some (Bauer et al., 2019; IHME, 2020; Im et al., 2023; Lelieveld et al., 2019; Vohra et al., 2021) , and higher than at least one other (Partanen et al., 2018). GBD2019 found higher impacts than those found here, using the same CRFs but different $PM_{2.5}$ concentrations, and also including neonatal deaths (IHME, 2020). The number of present-day respiratory deaths attributed here to O_3 exposure is generally higher than found in previous studies, e.g. (Anenberg et al., 2010; Silva et al., 2016) which both used an earlier, smaller CRF (Jerrett et al., 2009) than that used here. Studies utilising the CRFs used in this study (Turner et al., 2016) also find lower numbers of deaths than estimated here (GBD 2019 Risk Factors Collaborators, 2020; Malley et al., 2017; Shindell et al., 2018) , likely due to higher O_3 concentrations in UKESM1 (see Section 2).

The uncertainty in deaths due to the CRF (Table 1) is far larger than that from intra-ensemble pollutant variations for both $PM_{2.5}$ and O_3, consistent with prior studies determining the CRF to be the largest source of uncertainty (Johnston et al., 2012; Li et al., 2016; Shindell et al., 2018; S. T. Turnock et al., 2016).

https://doi.org/10.5194/egusphere-2023-2037
Preprint. Discussion started: 19 September 2023

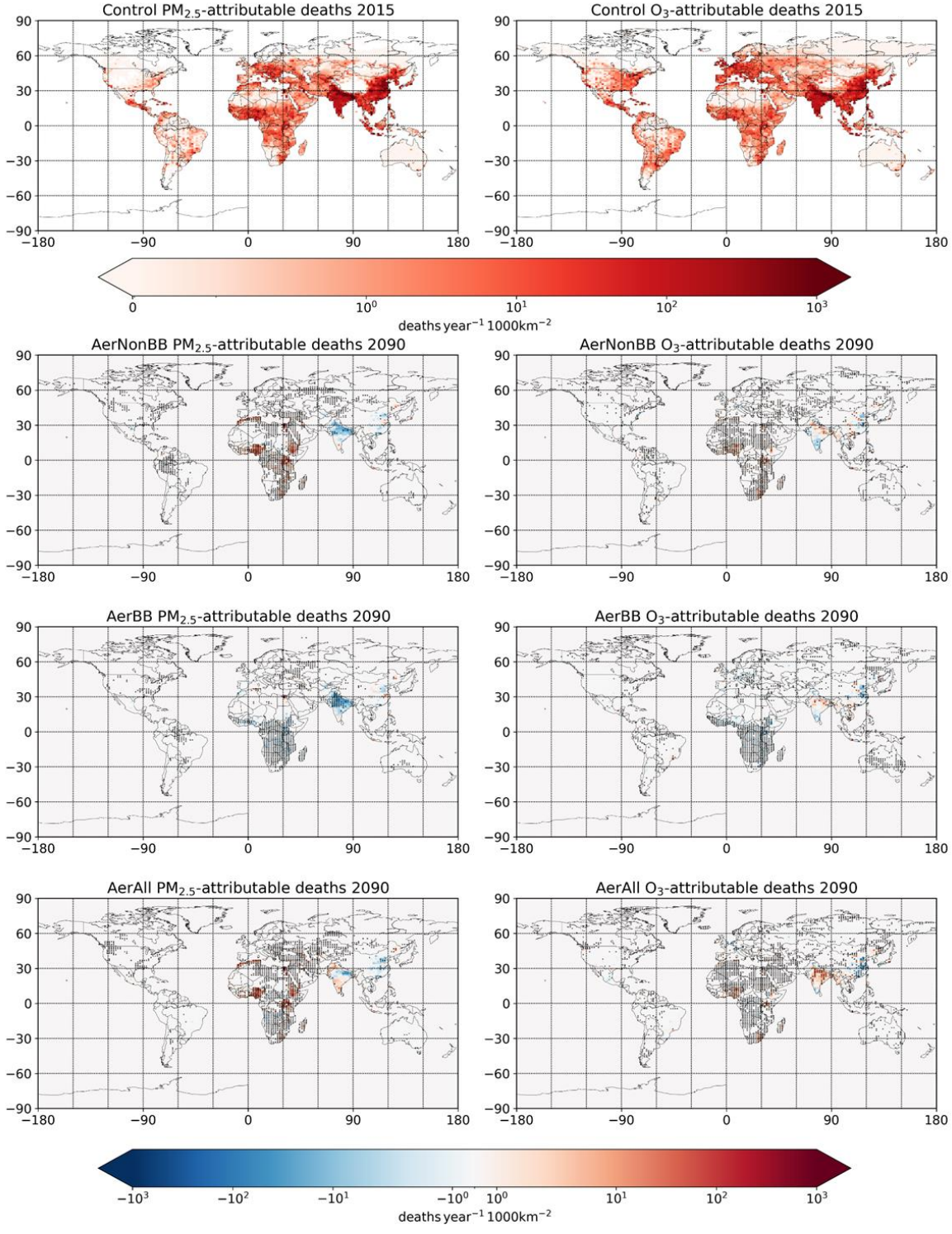

https://doi.org/10.5194/egusphere-2023-2037
Preprint. Discussion started: 19 September 2023

Figure 2: Top row: annual deaths per 1000km^2 attributable to air pollution for all CODs for $PM_{2.5}$ and respiratory illnesses for O_3 in 2015. Subsequent rows: impact of each scenario on 2090 deaths per 1000km^2 attributable to $PM_{2.5}$ and O_3 exposure relative to the SSP119 control, using 2015 spatial and age-based population distributions. Stippling indicates areas where the change is greater than one intra-ensemble standard deviation away from zero.

Species	Region	COD	Mean (thousand deaths/yr)	Low RR (thousand deaths/yr)	High RR (thousand deaths/yr)
$PM_{2.5}$	Global	All	2760 ± 30	2110 ± 30	3480 ± 30
		COPD	310 ± 4	245 ± 4	377 ± 4
		IHD	920 ± 10	697 ± 9	1190 ± 10
		LC	196 ± 3	148 ± 3	247 ± 3
		Stroke	870 ± 10	690 ± 10	1060 ± 10
		T2DM	197 ± 1	145 ± 1	254 ± 1
		LRI	264 ± 6	184 ± 5	361 ± 8
$PM_{2.5}$	Africa	All	340 ± 10	250 ± 10	430 ± 10
	Europe		58 ± 6	22 ± 3	111 ± 9
	Asia		2180 ± 30	1730 ± 20	2660 ± 30
	Central Africa		43 ± 2	33 ± 2	54 ± 2
O_3	Global	Resp	2280 ± 30	1730 ± 30	2700 ± 30
	Global 31.1ppb		2160 ± 30	1630 ± 30	2570 ± 40
	Africa		169 ± 3	125 ± 3	204 ± 4
	Europe		139 ± 5	100 ± 3	172 ± 5
	Asia		1680 ± 30	1290 ± 20	1970 ± 30
	Central Africa		29 ± 1	22 ± 1	34 ± 1

Table 1: Annual of deaths (in thousands) in 2015 attributable to $PM_{2.5}$, shown globally in total and for each COD separately, and the total across several regions (definitions in Figure S2), and those attributable to respiratory illnesses caused by O_3 exposure globally and in several regions. Also shown is the effect of using a Low Concentration Threshold (LCT, above which no harm is assumed; see Section 2) of 31.1ppb on global deaths for O_3, instead of the 26.7ppb used for the main results. Values are shown using the central CRF estimate and the 5th and 95th percentiles. The uncertainty given for each estimate is the estimated 5-95 percentile range across the ten control ensemble members, calculated as the standard deviation multiplied by 1.6449. The region definitions are shown in Figure S2.

https://doi.org/10.5194/egusphere-2023-2037
Preprint. Discussion started: 19 September 2023

The 2nd to 4th rows of Figure 2 show the effect on annual deaths per 1000 km^2 in 2090 of the different emissions scenarios, relative to the SSP119 control scenario, for both $PM_{2.5}$ and O_3. Population distributions from 2015 are used here to isolate the effect of the changed pollutants. The spatial pattern of human health impacts is broadly consistent with the emissions changes, modulated by the population distribution. AerNonBB features higher deaths across Africa than in the control, particularly in the highly populated West and East regions, due to future increases in fossil-fuel emissions. The decrease in dust emissions in the southern Sahara leads to an overall reduction in $PM_{2.5}$ (and hence deaths) in this region, indicating that indirect effects of pollutant emissions on atmospheric circulation and therefore natural emissions can have a substantial influence on their overall impact (Bauer et al., 2019). The lower future African biomass burning emissions in the AerBB experiment compared to the control result in significantly lower deaths across central and southern Africa. Still, the co-location of fossil fuel emissions with population centres causes these emissions to dominate the overall impact in AerAll.

Some remote impacts of the changed emissions are visible, with Southern Europe and the Middle East exhibiting consistent changes with those found in North Africa. The impact in each scenario relative to the control on global and African $PM_{2.5}$ and O_3 annual deaths in 2090 is shown in Table 2, and the total deaths are shown in Figure 3 over Africa and globally, with additional regions in the Supplement. Overall, Africa following SSP370 rather than SSP119 emissions leads to around 150,000 additional annual deaths across Africa from $PM_{2.5}$, and 15,000 from O_3, when the background populations are held constant (1st column of Table 2). In Africa, air pollutant trends are consistent with the impact changes (Figure S3). O_3 is projected to approximately match $PM_{2.5}$ in its health impacts by 2090 in these scenarios, due to the weaker decline in O_3 levels than in $PM_{2.5}$ (Figure 3).

	$PM_{2.5}$		O_3	
	Global	Africa	Global	Africa
AerNonBB	**130**	**154**	**23**	**24**
AerBB	**-44**	-2	**-22**	**-18**
AerAll	**151**	**152**	**25**	**15**

Table 2: Effect of each scenario, relative to the control, in thousands of $PM_{2.5}$ and O_3 deaths in 2090 globally and over Africa, using 2015 populations. Values are bolded when they are more than one intra-ensemble standard deviation away from zero. The Africa region definition is shown in Figure S2.

https://doi.org/10.5194/egusphere-2023-2037
Preprint. Discussion started: 19 September 2023

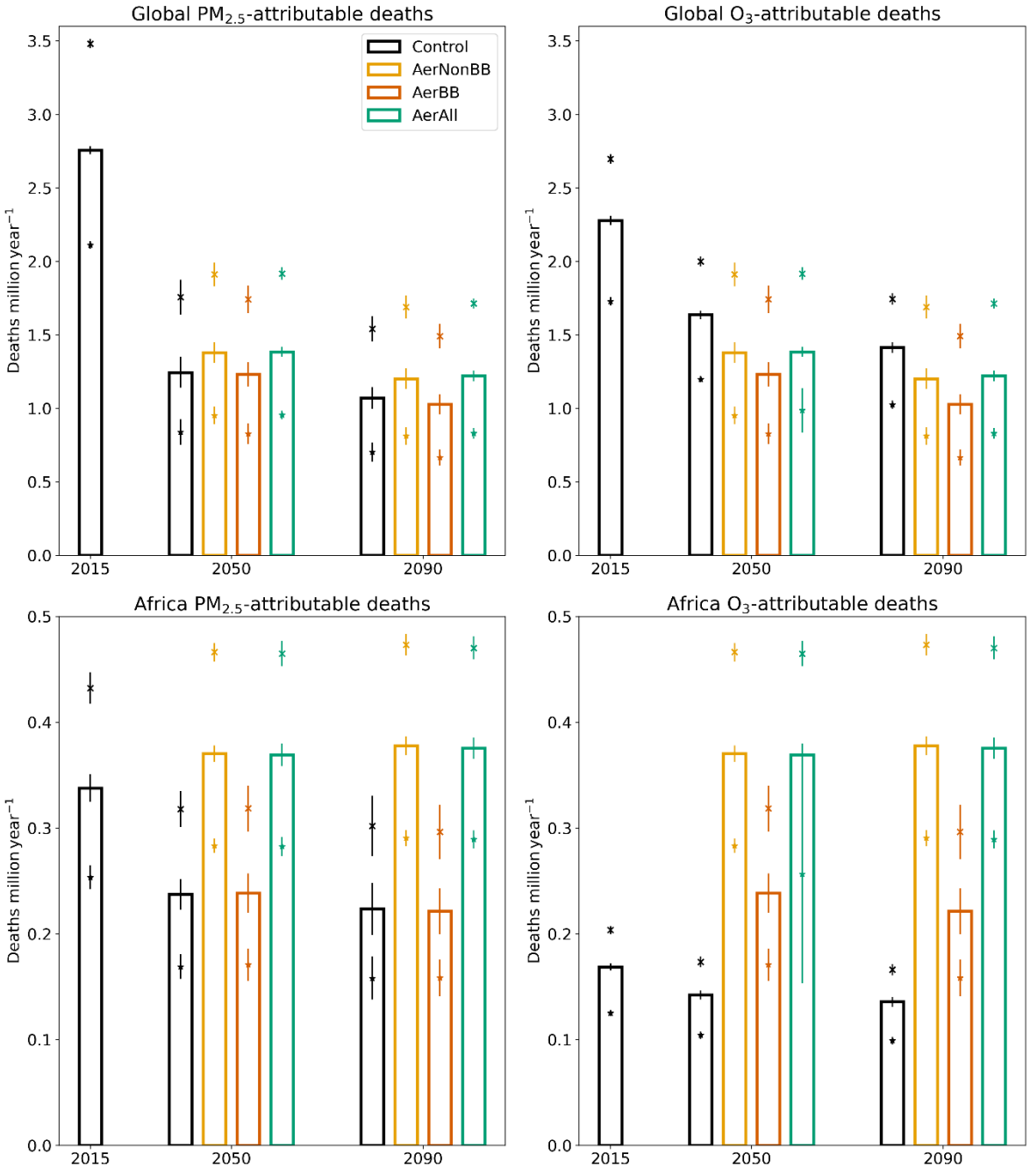

Figure 3: Annual $PM_{2.5}$- and O_3-attributable deaths in the control in 2015, and each scenario in 2050 and 2090, globally and over Africa, using 2015 spatial and age-based population distributions. The bars indicate the estimated deaths using the central CRF estimates; the crosses and stars use the 95th and 5th percentile CRF values respectively. For each CRF value, the (much smaller) uncertainty due to intra-ensemble variation in pollutant concentrations is indicated with vertical error bars. This intra-

https://doi.org/10.5194/egusphere-2023-2037
Preprint. Discussion started: 19 September 2023

ensemble variation is defined as the estimated 5-95 percentile range across the ten control ensemble members, calculated as the standard deviation multiplied by 1.6449. The Africa region definition is shown in Figure S2.

4 Discussion and Conclusions

This study used the Earth System Model UKESM1 to explore the range of impacts from future African pollutant emissions on air quality and premature mortality. The strong mitigation SSP119 scenario was compared to three alternative emissions scenarios, each substituting a subset of pollutant emissions over Africa for their (weak mitigation) SSP370 equivalent. Compared to SSP119, SSP370 has much higher fossil fuel and biofuel emissions, but lower African biomass burning emissions. The increase in non-biomass emissions far outweighs the decrease in biomass emissions, particularly over population centres. To evaluate the human health impacts of the future emissions, CRFs were used from the recent GBD2019 study (GBD 2019 Risk Factors Collaborators, 2020) for six CODs for $PM_{2.5}$, and (Turner et al., 2016) for O_3 Respiratory impacts. Estimates were calculated using present-day demographics, to isolate the effect of changes in pollutants on a given population.

Global deaths attributed to $PM_{2.5}$ and O_3 in 2015 were 2.76 (2.11 – 3.48) million and 2.28 (1.73 – 2.70) million respectively (5-95th percentile CRF uncertainties). While the differing methodology precludes an expectation of full consistency, the $PM_{2.5}$ value is comparable to – but generally slightly lower than – prior studies, and the O_3 value is larger than typically estimated, including in studies using the same CRFs. This is likely due to a positive bias in UKESM1's surface O_3 concentrations, especially in the tropics, but sparse observations preclude a full evaluation. The estimated O_3 impacts were not very sensitive to changes in the LCT. The dominance of the uncertainties in CRF over those in $PM_{2.5}$ concentrations is consistent with prior research (Shindell et al., 2018).

The effect of Africa following SSP370 rather than SSP119 is estimated to result in 150,000 additional annual deaths from $PM_{2.5}$, and 15,000 from O_3, across Africa in 2090, when using 2015 populations. Due to the large decrease in aerosol emissions in SSP119, annual $PM_{2.5}$ deaths could be similar to those due to O_3 by the end of the century. However, this result may also be affected by the O_3 biases.

Correcting for model biases in $PM_{2.5}$ and O_3 concentrations in a CMIP6 model with low-biased concentrations was found to substantially affect estimated health impacts (Im et al., 2023), though this effect was strongest over high emissions regions, and dampened when using more recent non-linear CRFs. The results of the scenarios in this study should therefore be primarily interpreted relative to each other, as the substantial differences between scenarios are less affected by the model biases.

Present-day populations were used in this study to isolate the effect of changes in air pollutants alone, and because of the difficulties in projecting changes in mortality rates. Increasing and ageing future populations will lead to higher estimated

https://doi.org/10.5194/egusphere-2023-2037
Preprint. Discussion started: 19 September 2023

deaths, and hence larger reductions in deaths upon emissions mitigation. In SSP1, the present-day African population of 1bn increases to around 1.7bn by 2070, before declining slightly; in SSP3, it increases throughout the century, reaching 4bn by 2090 (Lutz et al., 2018). Projected urbanisation (Jiang & O'Neill, 2017) will increase the co-location of population centres and emissions, increasing the human health impacts of air pollution (Silva et al., 2017). This co-location is already dampened by the coarse model grid, which reduces the estimated impacts (Li et al., 2016; Likhvar et al., 2015), an effect which will be more pronounced for $PM_{2.5}$ than for ozone (Malley et al., 2017). Prior work has found changes in populations play a comparable role to those in emissions in the SSPs (Im et al., 2023), though this estimate assumed the persistence of present-day baseline mortality rates.

Relatively higher non-BB aerosol south of the Sahara weakened the local surface circulation, reducing dust emissions sufficiently to reduce overall $PM_{2.5}$ levels (and hence deaths) in some areas, demonstrating the importance of accounting for natural aerosols and circulation impacts when estimating the impacts of emissions changes. This effect will likely vary substantially between models, due to differing aerosol impacts and parameterisations of dust emissions.

The CRFs used in this study are generated by combining multiple cohort studies (GBD 2019 Risk Factors Collaborators, 2020). The more recent CRFs used here cover a wider range of air pollutant concentrations than those in earlier studies, but there are still limitations in the representativeness of the input data. In particular, Africa is underrepresented in cohort studies (Chen & Hoek, 2020). If BC has a higher toxicity (Lelieveld et al., 2015), future air pollutant impacts per unit concentration change of $PM_{2.5}$ would be reduced as BC's share of $PM_{2.5}$ declines, and the effect of $PM_{2.5}$ mitigation therefore enhanced.

UKESM1's horizontal resolution is coarser than the relevant scales for localised air pollutants from different sources, as the distinction between rural/urban and emissions from vehicles, factories, and domestic fuel is dampened by averaging across the model gridcells. Global models are incapable of resolving these distinctions, which are of relevance for policy and behavioural considerations. Models of this resolution still clearly resolve distinctions between high and low air pollutant regions (Figure 1), and this method has been applied in many prior studies, often at coarser resolutions, to generate understandings of the global mortality impact of air pollution (Anenberg et al., 2010; Lelieveld et al., 2013, 2019; Partanen et al., 2018; Shindell et al., 2018; Silva et al., 2016, 2017; Vohra et al., 2021).

Pollutant concentrations from single years were used to estimate the health impacts (see Section 2). While the intra-ensemble mean was used, the variation in the concentrations manifests in large variations in the projected impacts over heavily populated regions which had no emissions change in our experiments, such as in Asia.

The effect of different future African emissions pathways on human health is large: reductions of anthropogenic African aerosol emissions through climate mitigation within the range of the SSPs can reduce annual deaths by 150,000 for $PM_{2.5}$, and 15,000 for O_3, compared to a more polluted pathway, using present-day demographics. These values can be expected to be

https://doi.org/10.5194/egusphere-2023-2037
Preprint. Discussion started: 19 September 2023

larger under future increasing and ageing populations. These results are focused on 2090, but the rapid emissions drop in SSP119 suggests that significant benefits would occur much faster under such a scenario. Substantial near-term localised reductions in the impacts of air pollution could therefore be obtained as co-benefits of climate change mitigation in Africa.

Data availability

Reasonable requests for model output and the data used for figures in this manuscript are available from the corresponding author.

Author contributions

AV and CDW conceived and designed the experiments. CDW carried out the analysis with assistance from MK and ME and led the preparation of the paper. All authors provided discussion of the analysis and reviewed the paper.

Competing interests

The authors declare that they have no conflict of interest.

Acknowledgements

This work was supported by the Natural Environment Research Council (grant number NE/L002515/1). AV and MK acknowledge the Leverhulme Trust (grant no. RC-2018-023) for providing funding through the Leverhulme Centre for Wildfires, Environment and Society. Simulations with UKESM1 were performed using the Monsoon2 system, a collaborative facility supplied under the Joint Weather and Climate Research Programme, which is a strategic partnership between the Met Office and the Natural Environment Research Council.

References

Allen, R. J., Horowitz, L. W., Naik, V., Oshima, N., O'Connor, F. M., Turnock, S., Shim, S., le Sager, P., van Noije, T., Tsigaridis, K., Bauer, S. E., Sentman, L. T., John, J. G., Broderick, C., Deushi, M., Folberth, G. A., Fujimori, S., & Collins, W. J. (2021). Significant climate benefits from near-term climate forcer mitigation in spite of aerosol reductions. *Environmental Research Letters*, *16*, 034010. https://doi.org/10.1088/1748-9326/abe06b

Anenberg, S. C., Horowitz, L. W., Tong, D. Q., & West, J. J. (2010). An estimate of the global burden of anthropogenic ozone and fine particulate matter on premature human mortality using atmospheric modeling. *Environmental Health Perspectives*, *118*(9), 1189–1195. https://doi.org/10.1289/ehp.0901220

Archibald, A. T., M O'Connor, F., Luke Abraham, N., Archer-Nicholls, S., P Chipperfield, M., Dalvi, M., A Folberth, G., Dennison, F., S Dhomse, S., T Griffiths, P., Hardacre, C., J Hewitt, A., S Hill, R., E Johnson, C., Keeble, J., O Köhler, M., Morgenstern, O., P Mulcahy, J., Ordóñez, C., … Zeng, G. (2020). Description and evaluation of the UKCA

https://doi.org/10.5194/egusphere-2023-2037
Preprint. Discussion started: 19 September 2023

stratosphere-troposphere chemistry scheme (StratTrop vn 1.0) implemented in UKESM1. *Geoscientific Model Development*, *13*(3), 1223–1266. https://doi.org/10.5194/gmd-13-1223-2020

Bauer, S. E., Im, U., Mezuman, K., & Gao, C. Y. (2019). Desert Dust, Industrialization, and Agricultural Fires: Health Impacts of Outdoor Air Pollution in Africa. *Journal of Geophysical Research: Atmospheres*, *124*(7), 4104–4120. https://doi.org/10.1029/2018JD029336

Bellouin, N., Mann, G. W., Woodhouse, M. T., Johnson, C., Carslaw, K. S., & Dalvi, M. (2013). Impact of the modal aerosol scheme GLOMAP-mode on aerosol forcing in the hadley centre global environmental model. *Atmospheric Chemistry and Physics*, *13*, 3027–3044. https://doi.org/10.5194/acp-13-3027-2013

Bellouin, N., Rae, J., Jones, A., Johnson, C., Haywood, J., Boucher, O., Bellouin, C. :, Rae, J., Jones, A., Johnson, C., Haywood, J., & Boucher, O. (2011). Aerosol forcing in the Climate Model Intercomparison Project (CMIP5) simulations by HadGEM2-ES and the role of ammonium nitrate. *Journal of Geophysical Research: Atmospheres*, *116*(D20), 20206. https://doi.org/10.1029/2011JD016074

Burnett, R., Chen, H., Szyszkowicza, M., Fann, N., Hubbell, B., III, C. A. P., Apte, J. S., Brauer, M., Cohen, A., Weichenthal, S., Coggins, J., Di, Q., Brunekreef, B., Frostad, J., Lim, S. S., Kan, H., Walker, K. D., Thurston, G. D., Hayes, R. B., … Spadaro, J. v. (2018). Global estimates of mortality associated with long-term exposure to outdoor fine particulate matter. *Proceedings of the National Academy of Sciences*, *115*(38), 9592–9597. https://doi.org/10.1073/pnas.1803222115

Burnett, R. T., Pope, C. A., Ezzati, M., Olives, C., Lim, S. S., Mehta, S., Shin, H. H., Singh, G., Hubbell, B., Brauer, M., Anderson, H. R., Smith, K. R., Balmes, J. R., Bruce, N. G., Kan, H., Laden, F., Prüss-Ustün, A., Turner, M. C., Gapstur, S. M., … Cohen, A. (2014). An integrated risk function for estimating the global burden of disease attributable to ambient fine particulate matter exposure. *Environmental Health Perspectives*, *122*(4), 397–403. https://doi.org/10.1289/ehp.1307049

Chen, J., & Hoek, G. (2020). Long-term exposure to PM and all-cause and cause-specific mortality: A systematic review and meta-analysis. *Environment International*, *143*, 105974. https://doi.org/10.1016/j.envint.2020.105974

CIESIN. (2018). Gridded Population of the World, Version 4 (GPWv4): Administrative Unit Center Points with Population Estimates, Revision 11. *Center for International Earth Science Information Network (CIESIN)*.

Ezzati, M., Lopez, A. D., Rogers, A., & Murray, C. J. L. (2004). Comparative Quantification of Health Risks: Global and Regional Burden of Disease Attributable to Selected Major Risk Factors. *World Health Organization*.

Fujimori, S., Hasegawa, T., Masui, T., Takahashi, K., Herran, D. S., Dai, H., Hijioka, Y., & Kainuma, M. (2017). SSP3: AIM implementation of Shared Socioeconomic Pathways. *Global Environmental Change*, *42*, 268–283. https://doi.org/10.1016/j.gloenvcha.2016.06.009

GBD 2019 Risk Factors Collaborators. (2020). Global burden of 87 risk factors in 204 countries and territories, 1990–2019: a systematic analysis for the Global Burden of Disease Study 2019. *The Lancet*, *396*, 1223–1249. https://doi.org/10.1016/S0140-6736(20)30752-2

https://doi.org/10.5194/egusphere-2023-2037
Preprint. Discussion started: 19 September 2023

Gidden, M. J., Riahi, K., Smith, S. J., Fujimori, S., Luderer, G., Kriegler, E., van Vuuren, D. P., van den Berg, M., Feng, L., Klein, D., Calvin, K., Doelman, J. C., Frank, S., Fricko, O., Harmsen, M., Hasegawa, T., Havlik, P., Hilaire, J., Hoesly, R., … Takahashi, K. (2019). Global emissions pathways under different socioeconomic scenarios for use in CMIP6: a dataset of harmonized emissions trajectories through the end of the century. *Geosci. Model Dev*, *12*, 1443–1475. https://doi.org/10.5194/gmd-12-1443-2019

Gidden, M., Riahi, K., Smith, S., Fujimori, S., Luderer, G., Kriegler, E., van Vuuren, D., van den Berg, M., Feng, L., Klein, D., Calvin, K., Doelman, J., Frank, S., Fricko, O., Harmsen, M., Hasegawa, T., Havlik, P., Hilaire, J., Hoesly, R., … Takahashi, K. (2018). *input4MIPs.CMIP6.ScenarioMIP.IAMC.IAMC-IMAGE-ssp119-1-1*. https://doi.org/10.22033/ESGF/input4MIPs.2485

Gliß, J., Mortier, A., Schulz, M., Andrews, E., Balkanski, Y., Bauer, S. E., Benedictow, A. M. K., Bian, H., Checa-Garcia, R., Chin, M., Ginoux, P., Griesfeller, J. J., Heckel, A., Kipling, Z., Kirkevåg, A., Kokkola, H., Laj, P., le Sager, P., Lund, M. T., … Tsyro, S. G. (2021). AeroCom phase III multi-model evaluation of the aerosol life cycle and optical properties using ground- and space-based remote sensing as well as surface in situ observations. *Atmospheric Chemistry and Physics*, *21*, 87–128. https://doi.org/10.5194/acp-21-87-2021

IHME. (2020). GBD Compare Data Visualization. *Institute for Health Metrics and Evaluation (IHME)*.

Im, U., Bauer, S. E., Frohn, L. M., Geels, C., Tsigaridis, K., & Brandt, J. (2023). Present-day and future $PM_{2.5}$ and O_3-related global and regional premature mortality in the EVAv6.0 health impact assessment model. *Environmental Research*, *216*. https://doi.org/10.1016/j.envres.2022.114702

Jerrett, M., Burnett, R. T., III, C. A. P., Ito, K., Thurston, G., Krewski, D., Shi, Y., Calle, E., & Thun, M. (2009). Long-Term Ozone Exposure and Mortality. *N Engl J Med*, *360*(11), 1085–1095. https://doi.org/10.1038/jid.2014.371

Jiang, L., & O'Neill, B. C. (2017). Global urbanization projections for the Shared Socioeconomic Pathways. *Global Environmental Change*, *42*, 193–199. https://doi.org/10.1016/J.GLOENVCHA.2015.03.008

Johnston, F. H., Henderson, S. B., Chen, Y., Randerson, J. T., Marlier, M., DeFries, R. S., Kinney, P., Bowman, D. M. J. S., & Brauer, M. (2012). Estimated global mortality attributable to smoke from landscape fires. *Environmental Health Perspectives*, *120*(5), 695–701. https://doi.org/10.1289/ehp.1104422

Kasoar, M., Shawki, D., & Voulgarakis, A. (2018). Similar spatial patterns of global climate response to aerosols from different regions. *Npj Climate and Atmospheric Science*, *1*(12). https://doi.org/10.1038/s41612-018-0022-z

Lelieveld, J., Barlas, C., Giannadaki, D., & Pozzer, A. (2013). Model calculated global, regional and megacity premature mortality due to air pollution. *Atmospheric Chemistry and Physics*, *13*(14), 7023–7037. https://doi.org/10.5194/acp-13-7023-2013

Lelieveld, J., Evans, J. S., Fnais, M.Giannadaki, D., & Pozzer, A. (2015). The contribution of outdoor air pollution sources to premature mortality on a global scale. *Nature*, *525*, 367–371. https://doi.org/10.1038/nature15371

https://doi.org/10.5194/egusphere-2023-2037
Preprint. Discussion started: 19 September 2023

Lelieveld, J., Klingmüller, K., Pozzer, A., Burnett, R. T., Haines, A., & Ramanathan, V. (2019). Effects of fossil fuel and total anthropogenic emission removal on public health and climate. *Proceedings of the National Academy of Sciences*, *116*(15), 7192–7197. https://doi.org/10.1073/pnas.1819989116

Li, Y., Henze, D. K., Jack, D., & Kinney, P. L. (2016). The influence of air quality model resolution on health impact assessment for fine particulate matter and its components. *Air Quality, Atmosphere and Health*, *9*, 51–68. https://doi.org/10.1007/s11869-015-0321-z

Likhvar, V. N., Pascal, M., Markakis, K., Colette, A., Hauglustaine, D., Valari, M., Klimont, Z., Medina, S., & Kinney, P. (2015). A multi-scale health impact assessment of air pollution over the 21st century. *Science of the Total Environment*, *514*, 439–449. https://doi.org/10.1016/j.scitotenv.2015.02.002

Liu, L., Shawki, D., Voulgarakis, A., Kasoar, M., Samset, B. H., Myhre, G., Forster, P. M., Hodnebrog, Sillmann, J., Aalbergsjø, S. G., Boucher, O., Faluvegi, G., Iversen, T., Kirkevåg, A., Lamarque, J. F., Olivié, D., Richardson, T., Shindell, D., & Takemura, T. (2018). A PDRMIP Multimodel study on the impacts of regional aerosol forcings on global and regional precipitation. *Journal of Climate*, *31*(11), 4429–4447. https://doi.org/10.1175/JCLI-D-17-0439.1

Lutz, W., Goujon, A., Kc, S., Stonawski, M., & Stilianakis, N. (2018). Demographic and Human Capital Scenarios for the 21st Century: 2018 assessment for 201 countries. *Publications Office of the European Union*.

Malley, C. S., Henze, D. K., Kuylenstierna, J. C. I., Vallack, H. W., Davila, Y., Anenberg, S. C., Turner, M. C., & Ashmore, M. R. (2017). Updated global estimates of respiratory mortality in adults ≥ 30 years of age attributable to long-term ozone exposure. *Environmental Health Perspectives*, *125*(8). https://doi.org/10.1289/EHP1390

Mansournia, M. A., & Altman, D. G. (2018). Population attributable fraction. *BMJ*, *360*(k757). https://doi.org/10.1136/BMJ.K757

Mulcahy, J., Johnson, C., Jones, C., Povey, A., Scott, C., Sellar, A., Turnock, S., Woodhouse, M., Abraham, N. L., Andrews, M., Bellouin, N., Browse, J., Carslaw, K., Dalvi, M., Folberth, G., Glover, M., Grosvenor, D., Hardacre, C., Hill, R., … Yool, A. (2020). Description and evaluation of aerosol in UKESM1 and HadGEM3-GC3.1 CMIP6 historical simulations. *Geoscientific Model Development Discussions*, *13*(12), 6383–6423. https://doi.org/10.5194/gmd-2019-357

O'Neill, B. C., Kriegler, E., Ebi, K. L., Kemp-Benedict, E., Riahi, K., Rothman, D. S., van Ruijven, B. J., van Vuuren, D. P., Birkmann, J., Kok, K., Levy, M., & Solecki, W. (2017). The roads ahead: Narratives for shared socioeconomic pathways describing world futures in the 21st century. *Global Environmental Change*, *42*, 169–180. https://doi.org/10.1016/j.gloenvcha.2015.01.004

Partanen, A.-I., Landry, J.-S., & Matthews, D. (2018). Climate and health implications of future aerosol emission scenarios. *Environmental Research Letters*, *13*(2), 024028. https://doi.org/10.1088/1748-9326/aaa511

Persad, G. G., & Caldeira, K. (2018). Divergent global-scale temperature effects from identical aerosols emitted in different regions. *Nature Communications*, *9*(3289). https://doi.org/10.1038/s41467-018-05838-6

https://doi.org/10.5194/egusphere-2023-2037
Preprint. Discussion started: 19 September 2023

Pope III, C. A., Burnett, R. T., Krewski, D., Jerrett, M., Shi, Y., Calle, E. E., & Thun, M. J. (2009). Cardiovascular Mortality and Exposure to Airborne Fine Particulate Matter and Cigarette Smoke. *Circulation*, *120*(11), 941–948. https://doi.org/10.1161/circulationaha.109.857888

Pope III, C. A., Burnett, R. T., Thun, M. J., Calle, E. E., Krewski, D., Ito, K., & Thurston, G. D. (2002). Lung Cancer, Cardiopulmonary Mortality, and Long-term Exposure to Fine Particulate Air Pollution. *Jama*, *287*(9), 1132–1141. https://doi.org/10.1001/jama.287.9.1132

Sandvik, B. (2008). World Borders Dataset. *Thematic Mapping*. http://thematicmapping.org/downloads/world_borders.php

Schucht, S., Colette, A., Rao, S., Holland, M., Schöpp, W., Kolp, P., Klimont, Z., Bessagnet, B., Szopa, S., Vautard, R., Brignon, J.-M., & Rouïl, L. (2015). Moving towards ambitious climate policies: Monetised health benefits from improved air quality could offset mitigation costs in Europe. *Environmental Science and Policy*, *50*, 252–269. https://doi.org/10.1016/j.envsci.2015.03.001

Sellar, A. A., Jones, C. G., Mulcahy, J. P., Tang, Y., Yool, A., Wiltshire, A., O'Connor, F. M., Stringer, M., Hill, R., Palmieri, J., Woodward, S., de Mora, L., Kuhlbrodt, T., Rumbold, S. T., Kelley, D. I., Ellis, R., Johnson, C. E., Walton, J., Abraham, N. L., … Zerroukat, M. (2019). UKESM1: Description and Evaluation of the U.K. Earth System Model. *Journal of Advances in Modeling Earth Systems*, *11*(12), 4513–4558. https://doi.org/10.1029/2019MS001739

Shawki, D., Voulgarakis, A., Chakraborty, A., Kasoar, M., & Srinivasan, J. (2018). The South Asian Monsoon Response to Remote Aerosols: Global and Regional Mechanisms. *Journal of Geophysical Research: Atmospheres*, *123*, 11,511-11,601. https://doi.org/https://doi.org/10.1029/2018JD028623

Shindell, D., Faluvegi, G., Seltzer, K., & Shindell, C. (2018). Quantified, localized health benefits of accelerated carbon dioxide emissions reductions. *Nature Climate Change*, *8*, 291–295. https://doi.org/10.1038/s41558-018-0108-y

Silva, R. A., West, J. J., Lamarque, J. F., Shindell, D. T., Collins, W. J., Dalsoren, S., Faluvegi, G., Folberth, G., Horowitz, L. W., Nagashima, T., Naik, V., Rumbold, S. T., Sudo, K., Takemura, T., Bergmann, D., Cameron-Smith, P., Cionni, I., Doherty, R. M., Eyring, V., … Zengast, G. (2016). The effect of future ambient air pollution on human premature mortality to 2100 using output from the ACCMIP model ensemble. *Atmospheric Chemistry and Physics*, *16*(15), 9847–9862. https://doi.org/10.5194/acp-16-9847-2016

Silva, R. A., West, J. J., Lamarque, J. F., Shindell, D. T., Collins, W. J., Faluvegi, G., Folberth, G. A., Horowitz, L. W., Nagashima, T., Naik, V., Rumbold, S. T., Sudo, K., Takemura, T., Bergmann, D., Cameron-Smith, P., Doherty, R. M., Josse, B., MacKenzie, I. A., Stevenson, D. S., & Zeng, G. (2017). Future global mortality from changes in air pollution attributable to climate change. *Nature Climate Change*, *7*, 647–651. https://doi.org/10.1038/nclimate3354

Silva, R. A., West, J. J., Zhang, Y., Anenberg, S. C., Lamarque, J. F., Shindell, D. T., Collins, W. J., Dalsoren, S., Faluvegi, G., Folberth, G., Horowitz, L. W., Nagashima, T., Naik, V., Rumbold, S., Skeie, R., Sudo, K., Takemura, T., Bergmann, D., Cameron-Smith, P., … Zeng, G. (2013). Global premature mortality due to anthropogenic outdoor air pollution and the contribution of past climate change. *Environmental Research Letters*, *8*(3), 034005. https://doi.org/10.1088/1748-9326/8/3/034005

https://doi.org/10.5194/egusphere-2023-2037
Preprint. Discussion started: 19 September 2023

Smith, C. J., Kramer, R. J., Myhre, G., Alterskjr, K., Collins, W., Sima, A., Boucher, O., Dufresne, J. L., Nabat, P., Michou, M., Yukimoto, S., Cole, J., Paynter, D., Shiogama, H., M. O'Connor, F., Robertson, E., Wiltshire, A., Andrews, T., Hannay, C., … Forster, P. M. (2020). Effective radiative forcing and adjustments in CMIP6 models. *Atmospheric Chemistry and Physics*, *20*(16), 9591–9618. https://doi.org/10.5194/acp-20-9591-2020

Smith, K. R., & Peel, J. L. (2010). Mind the gap. *Environmental Health Perspectives*, *118*(12), 1643–1645. https://doi.org/10.1038/s41587-019-0141-z

Thornhill, G., Collins, W., Kramer, R., Olivié, D., O'Connor, F., Abraham, N., Bauer, S., Deushi, M., Emmons, L., Forster, P., Horowitz, L., Johnson, B., Keeble, J., Lamarque, J.-F., Michou, M., Mills, M., Mulcahy, J., Myhre, G., Nabat, P., … Zhang, J. (2021). Effective Radiative forcing from emissions of reactive gases and aerosols – a multimodel comparison. *Atmospheric Chemistry and Physics*, *21*(2), 853–874. https://doi.org/10.5194/acp-2019-1205

Turner, M. C., Jerrett, M., Pope, C. A., Krewski, D., Gapstur, S. M., Diver, W. R., Beckerman, B. S., Marshall, J. D., Su, J., Crouse, D. L., & Burnett, R. T. (2016). Long-Term Ozone Exposure and Mortality in a Large Prospective Study. *American Journal of Respiratory and Critical Care Medicine*, *193*(10), 1134–1142. https://doi.org/10.1164/rccm.201508-1633OC

Turnock, S., Allen, R., Andrews, M., Bauer, S., Emmons, L., Good, P., Horowitz, L., Michou, M., Nabat, P., Naik, V., Neubauer, D., O'Connor, F., Olivié, D., Schulz, M., Sellar, A., Takemura, T., Tilmes, S., Tsigaridis, K., Wu, T., & Zhang, J. (2020). Historical and future changes in air pollutants from CMIP6 models. *Atmospheric Chemistry and Physics*, *20*(23), 14547–14579. https://doi.org/10.5194/acp-2019-1211

Turnock, S. T., Butt, E. W., Richardson, T. B., Mann, G. W., Reddington, C. L., Forster, P. M., Haywood, J., Crippa, M., Janssens-Maenhout, G., Johnson, C. E., Bellouin, N., Carslaw, K. S., & Spracklen, D. v. (2016). The impact of European legislative and technology measures to reduce air pollutants on air quality, human health and climate. *Environmental Research Letters*, *11*(2), 024010. https://doi.org/10.1088/1748-9326/11/2/024010

van Vuuren, D. P., Stehfest, E., Gernaat, D. E. H. J., Doelman, J. C., van den Berg, M., Harmsen, M., de Boer, H. S., Bouwman, L. F., Daioglou, V., Edelenbosch, O. Y., Girod, B., Kram, T., Lassaletta, L., Lucas, P. L., van Meijl, H., Müller, C., van Ruijven, B. J., van der Sluis, S., & Tabeau, A. (2017). Energy, land-use and greenhouse gas emissions trajectories under a green growth paradigm. *Global Environmental Change*, *42*, 237–250. https://doi.org/10.1016/j.gloenvcha.2016.05.008

Vohra, K., Vodonos, A., Schwartz, J., Marais, E. A., Sulprizio, M. P., & Mickley, L. J. (2021). Global mortality from outdoor fine particle pollution generated by fossil fuel combustion: Results from GEOS-Chem. *Environmental Research*, *195*, 110754. https://doi.org/10.1016/j.envres.2021.110754

von Schneidemesser, E., Monks, P. S., Allan, J. D., Bruhwiler, L., Forster, P., Fowler, D., Lauer, A., Morgan, W. T., Paasonen, P., Righi, M., Sindelarova, K., & Sutton, M. A. (2015). Chemistry and the Linkages between Air Quality and Climate Change. *Chemical Reviews*, *115*(10), 3856–3897. https://doi.org/10.1021/acs.chemrev.5b00089

Wang, H., Xie, S. P., & Liu, Q. (2016). Comparison of climate response to anthropogenic aerosol versus greenhouse gas forcing: Distinct patterns. *Journal of Climate*, *29*(14), 5175–5188. https://doi.org/10.1175/JCLI-D-16-0106.1

https://doi.org/10.5194/egusphere-2023-2037
Preprint. Discussion started: 19 September 2023

Wells, C. D., Kasoar, M., Bellouin, N., & Voulgarakis, A. (2023). Local and remote climate impacts of future African aerosol emissions. *Atmospheric Chemistry and Physics*, *23*(6), 3575–3593. https://doi.org/10.5194/acp-23-3575-2023

World Health Organisation. (2021). *WHO global air quality guidelines: particulate matter (*$PM_{2.5}$ *and PM10), ozone, nitrogen dioxide, sulfur dioxide and carbon monoxide*. World Health Organization.